Materials synthesis using oxide free sol–gel systems†

Andrew L. Hector

Received 1st May 2007
First published as an Advance Article on the web 21st June 2007
DOI: 10.1039/b608838b

This *tutorial review* highlights some active areas of research into non-oxide sol–gel chemistry. These aim to capture some of the advantages of methods developed mainly with oxides for a new generation of functional materials based on main group and metal nitrides, and semiconducting chalcogenides. Sol–gel processing has a long track record in producing useful materials for optical, magnetic, electrical, catalytic and structural applications. Controlled morphologies can be produced on all lengths scales, from ordered mesoporous arrays to thin films, fibres and monoliths. Hence there is an opportunity to produce new morphologies in non-oxides and hence new applications of these materials.

1. Introduction

Sol–gel processes[1] allow formation of solid materials through gelation of solutions and can be used to produce a large number of useful morphologies, Fig. 1. A sol is usually defined as a stable suspension of particles or polymer molecules in a liquid, whereas a gel is obtained when interactions between species in the sol become extensive enough to immobilise the liquid.

In materials synthesis, gelation is usually due to the irreversible formation of covalent bonds. Gelation of the bulk solution results in monolithic materials and careful drying and firing can lead to high quality ceramic or glass bodies, alternatively supercritical solvent extraction can be used to make highly porous, low density monoliths.

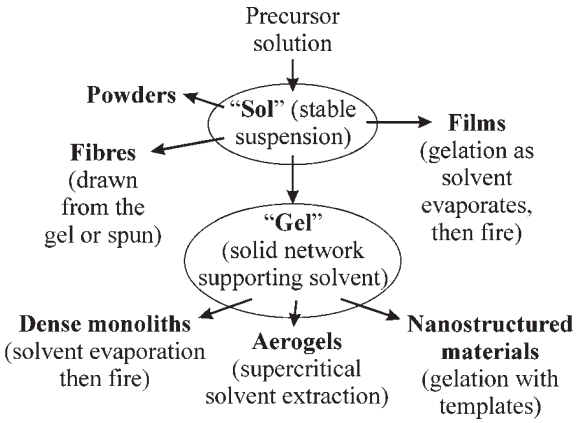

Fig. 1 Processing routes to materials using sol–gel methods.

Gelation during processing, usually with solvent evaporation, also yields useful materials. Spin- or dip-coated films gel during drying and can be fired to yield dense films, similarly spray drying can lead to spherical particles and spinning with evaporation to fibres. Moreover, in the presence of templating agents gelation can also enable the design of nanoporous materials and other useful nanostructures such as tubes, fibres, helices and ribbons.

Sol–gel methods have a strong track record in the production of oxide materials, where they were largely developed in the processing of silicate materials *via* silica gels.[1] These are often produced by hydrolysis and condensation of silicon alkoxides through nucleophilic substitution reactions, Fig. 2. These are catalysed by acid or base due to the poor nucleophilic properties of water and the steric effect of forming a 5-coordinate transition state with the small silicon atom.

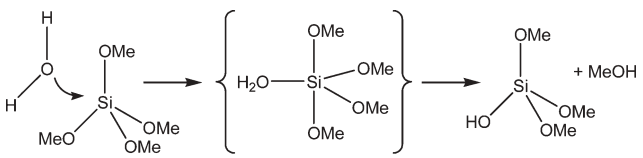

Fig. 2 Nucleophilic substitution of $Si(OMe)_4$ by water.

School of Chemistry, University of Southampton, Highfield, Southampton, UK SO17 1BJ. E-mail: A.L.Hector@soton.ac.uk; Fax: +44 (0) 2380596805; Tel: +44 (0) 2380594125
† The HTML version of this article has been enhanced with colour. images

Andrew L. Hector

Andrew Hector studied Chemistry at Imperial College, London, then obtained a PhD from University College London in 1995. After postdoctoral periods working on complex oxide fluorides and lithium battery cathode materials, he took up a Royal Society University Research Fellowship at the University of Southampton in October 2000. In December 2005 he was appointed to a lectureship in structural and materials chemistry. His current research interests focus on metal nitride chemistry, specifically nanoparticle synthesis, sol–gel methods and nanostructured materials.

Condensation proceeds *via* the attack of a hydroxide group produced in the hydrolysis step on a neighbouring silicon atom. The transition state is protonated under acid catalysis and deprotonated under base catalysis and this overall charge is stabilised by the donor properties of the ligands. The effect is to promote the growth of polymeric chains under acid conditions and of dense particles with base. Hence the conditions need to be chosen carefully to yield sols or gels with speciation appropriate to the materials application.

The main difference in oxide sol–gel processing with metals instead of silicon is the reactivity of the alkoxides.[1] Metals are less electronegative than silicon and hence more susceptible to nucleophilic attack. They are also larger, so the expansion of their coordination sphere occurs much more readily. The same approaches as with silicon are used, but reactivity must be controlled by using sterically crowded alkoxides (*e.g.* isopropoxide), and/or precursor/solvent systems in which extra ligands or oligomer formation blocks vacant coordination sites.[1]

Over the last decade, two areas of non-oxide sol–gel chemistry have been developed to the point at which they promise significant new materials applications. One of these is the formation of nitride materials. Nitrides are commonly produced as powders, which are then difficult to process due to high melting/sintering temperatures caused by strong interactions of constituent ions with the highly polarisable N^{3-}. Vapour deposition routes to nitride films are well developed and find useful roles in optical, electronics and engineering environments. For some main group nitrides, there are also good preceramic polymer routes to fibres and coatings. Sol–gel methods promise to yield new and exciting morphologies and compositions that cannot be accessed by these routes. Sol–gel processing of metal chalcogenide nanoparticles to enable semiconductor materials to be solution processed or produced in porous forms has also undergone a period of significant development. The aim of this article is to summarise the achievements of these techniques in materials synthesis and provide some thoughts about future prospects of these methods.

2. Synthesis of non-oxide materials from alkoxides

Often the preparation of non-oxide materials from alkoxides uses standard hydrolytic sol–gel processes, then takes the processed oxide product and converts it to a non-oxide material by heating in a reactive gas environment. For example, ZrN thin films have been produced by spin-coating a $Zr(O^nPr)_4$-derived sol then heating the product at 1400 °C in the presence of graphite.[2] Similarly, extrusion of cellulose acetate fibres into a tantalum ethoxide solution results in gel fibres than can be pyrolysed at high temperatures to fibres of TaC (carbothermal reduction of the oxide with carbon from the polymer at 1500 °C) or TaN (NH_3 at 1400 °C), Fig. 3.[3]

In an alternative approach, Kumta[4] has reacted early transition metal or aluminium alkoxides with H_2S or hydrazine to obtain precipitates which can be pyrolysed to metal sulfides or nitrides. These are referred to as *thio* or *hydrazide* sol–gel processes. In these reactions nucleophilic substitution of alkoxide groups by H_2S or hydrazine is required to remove the oxygen bound to the metal. The reaction of $Ti(O^iPr)_4$ with a large excess, 10 equivalents, of hydrazine in refluxing acetonitrile results in a solid in which 80% of the alkoxy groups have been replaced by hydrazides.[4] These powders could then be pyrolysed in Ar to produce TiN with a low oxygen content, demonstrating that it is possible to produce non-oxide materials from alkoxides without heating the products in a reactive atmosphere such as NH_3 or H_2S.

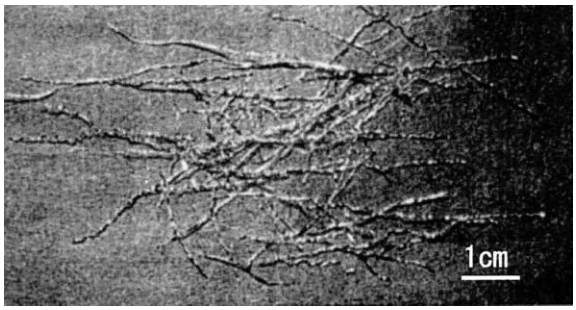

Fig. 3 TaN fibres produced from cellulose acetate–tantalum ethoxide gel at 1400 °C in NH_3. Reprinted from ref. 3, Copyright (2006), with permission from John Wiley and sons Inc.

There are two challenges in the use of oxygen-containing precursors that have led to the desire for oxygen-free precursor systems for sol–gel processing. The first is the concern that oxide will remain in the end products—in nitride materials produced from oxides the oxygen content can be significant even after long reaction times.[5] The second is that changes in morphology can be associated with the very high reaction temperatures that are often needed to replace oxide. Oxides often sinter readily at significantly lower temperatures than required to effect the transformation to non-oxide materials. Some of the useful morphologies that can be derived from sol–gel processing, including porous and nanostructured materials, cannot be converted to non-oxide materials in this way.

3. Sol–gel chemistry to produce silicon nitride and carbonitride materials

Non-oxidic routes to nitride materials have largely been developed with silicon and the formation of silicon nitrides using sol–gel chemistry has mainly been focused on two application areas, catalysis and ceramic materials.

It is straightforward to formulate a process based on ammonolysis of dialkylaminosilanes with ammonia followed by condensation to make imide (–NH–) linkages that is equivalent to the hydrolysis and condensation of alkoxides. However, the precursors and gels are highly air sensitive and the handling of these materials becomes much more difficult. The reaction shown in Scheme 1 has been used by Jansen[6] with $Si(NHMe)_4$ (see section 4.2) to make metal doped silicon nitrides. $Si(NMe_2)_3(NH_2)$ was developed by Bradley[7] as a precursor that would be able to undergo a condensation reaction without first needing ammonolysis, having noted that reactions of $Si(NR_2)_4$ with ammonia usually led to amorphous powders rather than gels.

$$Si(NR_2)_4 \xrightarrow{NH_3} Si(NH)_x(NH_2)_y(NR_2)_z \xrightarrow{heat} Si_3N_4$$

Scheme 1 An imide-based sol–gel route for silicon nitride.

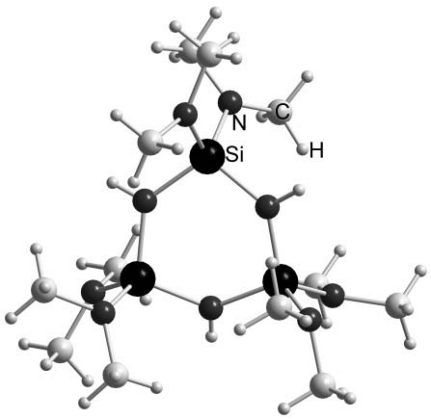

Fig. 4 Crystal structure of $[(Me_2N)_2Si(NH)]_3$.[7]

Addition of a catalytic quantity of trifluoromethanesulfonic acid to $Si(NMe_2)_3(NH_2)$ at 50 °C in THF results in self condensation with a cyclic silicon imide-dialkylamide species, Fig. 4, being the major product.[7] Exposure of this mixture to ammonia leads to gelation with loss of dimethylamine to give a semirigid, dimensionally stable, translucent gel. The effect of the acid is suggested to be the removal of NMe_2 groups as $HNMe_2$, resulting in precursor molecules containing triflate, an excellent leaving group for the ammonolysis and condensation reactions.[8] Presumably the electron withdrawing effect of a triflate group would also render the precursor molecule more susceptible to nucleophilic attack. Drying of gels produced using this chemistry under reduced pressure yielded a xerogel with a surface area of around 1000 m^2g^{-1}. Treatment with ammonia at 50 °C removes all traces of NMe_2 groups (according to IR spectra) resulting in amorphous $Si(NH)_x(NH_2)_y$ with a surface area of 500 m^2g^{-1}. The authors could not dry their monolithic gels without cracking.

Kroke and Riedel[9] have an entirely different approach, Scheme 2, which produces carbodiimide (Si–NCN–Si) linkages with the elimination of Me_3SiCl to yield gels that can be pyrolysed to silicon carbonitride. These silicon carbodiimide gels are immobile and undergo syneresis in exactly the same way as silica gels. Thus as further crosslinking occurs the gel body is seen to reduce in volume whilst retaining its shape and pore liquid is expelled. Gels produced by the acid catalysed ammonolysis of $Si(NMe_2)_3(NH_2)$ behave similarly.[7] Hence it is reasonable to suggest that these systems may provide a good route to shaped monolithic ceramics and also to aerogels once the drying processes can be controlled.

3.1 Porous silicon nitride and carbonitride membranes

Whilst monolithic gels could not be produced from the chemistry described in Scheme 1, mesoporous silicon nitride membranes could be produced[10] by dip coating a macroporous Al_2O_3 disk into a sol before gelation (sols were produced that were stable for 6 h). These membranes, after firing at 1000 °C in NH_3, were found to be effective gas filters, Fig. 5. Carbon

$$MeSiCl_3 \xrightarrow{(SiMe_3)_2NCN} MeSi(NCN)_{1.5} \xrightarrow{heat} Si(C,N)_z$$

Scheme 2 Carbodiimide-based sol–gel route for silicon nitride.

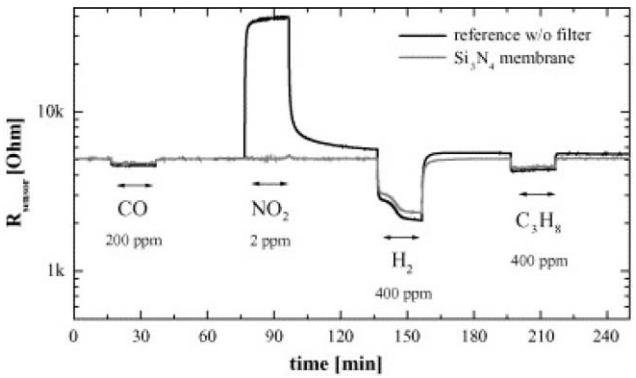

Fig. 5 Response of a broad band SnO_2 sensor to four gases with and without a mesoporous Si_3N_4 membrane. Reprinted from ref. 10, Copyright (2006), with permission from Elsevier.

dioxide, hydrogen and propane passed through the membranes readily but NO_2 was completely retarded. These are intended for use in selective gas sensor systems.

Silicon carbonitride membranes have also been produced using the carbodiimide route (Scheme 2), with the purpose of producing ceramic membranes with enhanced stability for high temperature applications.[11] To achieve this, the $MeSiCl_3$ in Scheme 2 was mixed with 10 equivalents of Me_2SiCl_2, so that croslinking was reduced and gelation did not go to completion. Hence a viscous material that was suitable for spin coating was obtained. When deposited on a macroporous Si_3N_4 substrate and pyrolysed at 1000 °C in Ar, a silicon carbonitride with 7–10 nm pores was obtained, this was suggested to be suitable for use as a catalyst support in high temperature membrane reactors.

3.2 Porous materials for catalysis

Silicon nitrides are of strong interest as heterogeneous catalysts,[12] as solid base catalysts in Knoevenagel reactions such as the condensation of benzaldehyde with malonitrile and (after impregnation with K) as efficient solid superbase catalysts. Kaskel[12] has demonstrated that the pore size (5.6–9.1 nm) and nitride/imide ratio can be controlled in mesoporous silicon imidonitride materials made from the solution phase reactions of $SiCl_4$ with ammonia followed by firing. Reactions of $Si(Me_2N)_3(NH_2)$ with ammonia in hot, concentrated solutions of long chain amines have been used to produce templated gels.[13] Careful pyrolysis in NH_3 yields microporous materials with narrow pore size distributions which can be controlled by the amine choice as shown in Table 1.

Table 1 Variation in pore size of templated silicon imidonitride catalysts with the template chain length[12]

Template	Average pore diameter/Å
$C_{12}H_{25}NH_2$	11.8
$C_{13}H_{27}NH_2$	12.4
$C_{14}H_{29}NH_2$	13.6
$C_{15}H_{31}NH_2$	13.7
$C_{16}H_{33}NH_2$	15.7
$C_{18}H_{37}NH_2$	16.5

A series of reactions was performed with micro- (1.7 nm) and mesoporous (5.6 nm) silicon imidonitride catalysts to demonstrate shape selectivity with these materials.[13] Alkylation of styrene with ethene proceeded smoothly with both materials to yield propylbenzene and (1-ethylpropyl)benzene. The microporous material was significantly more successful, achieving 74% conversion compared with 25% with the mesoporous catalyst. However, alkylation of benzene with styrene produced 100% conversion in 10 minutes with the mesoporous material but no conversion with the microporous one because the products are too large for the pores. Isomerisation of 1 : 1 mixtures of 1-hexene and 1-hexadecene was also investigated. Here the mesoporous material had significantly higher activity, but the microporous one was entirely selective for the isomerisation of 1-hexene. The more subtle differences between the different pore sizes available within the microporous and mesoporous systems are yet to be fully explored, but it is likely that some interesting selectivities might be discovered.

4. Other elements doped into silicon nitride

Virtually all elements other than silicon which would be of interest in nitride materials processed using sol–gel techniques are less electronegative than silicon. Most are also larger and hence will expand their coordination spheres more readily. Hence the reactivity of precursors will tend to be higher and their exposure to NH_3, or to other crosslinking agents such as $(Me_3Si)_2NCN$, often leads to precipitation. Hence non-oxide sol–gel methods are less well developed to nitrides of other elements.

One approach to this problem has been to dope other elements into silicon precursors such that the chemistry of the sol–gel process is essentially silicon based. Others have produced mixed element nitrides by balancing reaction rates of a silicon amide and another element amide with ammonia. Either way, the aim is to produce materials in which the properties of the silicon nitride host are augmented.

4.1 Si/B/C/N ceramics—structural materials from sol–gel and preceramic polymer routes

Silicon boron carbonitride ceramics are readily processed using sol–gel or preceramic polymer technology. These have strong prospects as low density (*i.e.* light), strong, tough materials with high resistance to thermal shock, corrosion and creep. Remarkably some Si/B/C/N materials are thermally stable to 2000 °C without mass loss or oxidative damage[14] and these ceramics have been used as oxidation/corrosion inhibiting coatings for other non-oxide materials.

Often, the chemistry used in sol–gel methods and preceramic polymers is similar and the main difference is in the processing. When polymers are used, the aim is to make a substance that is melt or solution processable to make fibres, films, monoliths *etc.* which then decomposes with retention of the desired morphology when pyrolysed in an appropriate gas environment.[15] The sol–gel approach often produces similar species in solution but these develop during the processing of the material.

Silicon boron nitride preceramic precursors for polymer processing are often made by linking $Cl_3Si–NH–BCl_2$ molecules with ammonia *via* HCl elimination.[16] The products make very good ceramic fibres of compositions such as $Si_3B_3N_7$ or $SiBN_3C$. These have high strength at very high temperatures, even in oxidising conditions, and are of interest for composite materials in applications such as gas turbines and jet propulsion engines. Interestingly, modelling studies showed that the cation distribution becomes heterogeneous on short length scales even when such a precursor, with Si and B already linked, is used.

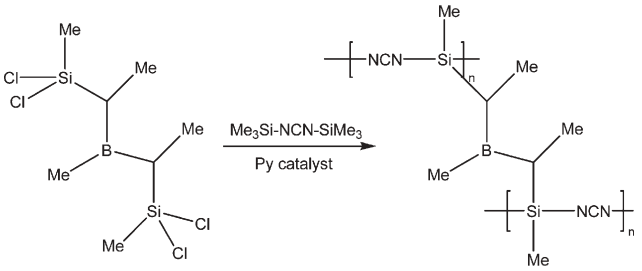

Fig. 6 Boron-modified carbodiimide sol–gel process.[17]

Weinmann[17] adapted the carbodiimide route discussed in section 3 to introduce boron into the gels, Fig. 6. In this case the products were milled to powders but then showed good properties during powder processing to produce dense ceramic monoliths.

Lithiation of $Si(NMe_2)_3(NH_2)$ with BuLi results in a precursor that can react with boron halides yielding Si–N–B bonds. This has been reacted[8] with BCl_3 or cyclic borazines to make precursors containing a 3 : 1, 1 : 1 or 2 : 3 ratio of Si : B, Fig. 7. These precursors have the same peripheral groups available for substitution with NH_3 as the cyclic silicon imide-amide shown in Fig. 4. Treatment of these precursors with ammonia in THF with a trifluoromethane sulfonic acid catalyst led to rigid or semirigid gels. Pyrolysis under N_2 at 1000 °C gave mesoporous solids with high surface areas and no free carbon.

It is clear that the properties of these promising ceramic materials vary extensively with the ratio of constituent

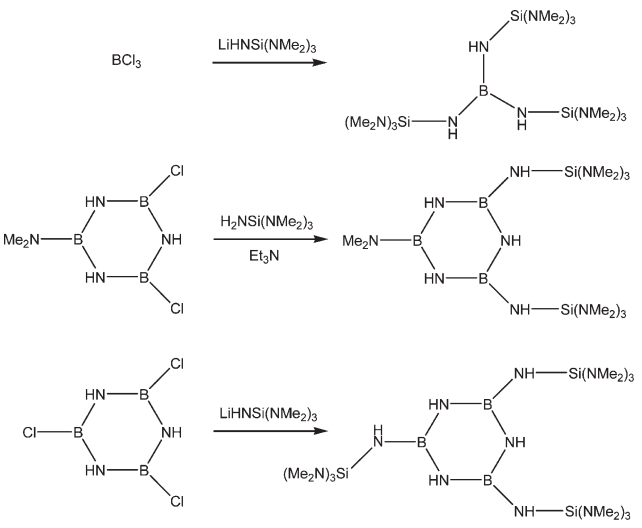

Fig. 7 Cyclic borazine precursors to Si/B/N gels.[8]

elements, but also with the atomic scale distribution. One of the major advantages of sol–gel or polymer routes to the mixed Si/B materials is this atomic scale mixing and the effect of small Si- or B- rich regions within these ceramics is yet to be fully understood. Hence this area of materials science is well served by the availability of a series of different chemical approaches that will produce subtly different materials for investigation of their properties.

4.2 Metal-doped silicon nitrides

There is also an interest in making aluminium–silicon nitrides for the same purposes of modifying the properties of silicon nitride. $Al(HNSi(NMe_2)_3)_3$ was prepared by the same method as the boron analogue, Fig. 7. It has also very similar gelation behaviour resulting in amorphous, mesoporous Si/Al/N ceramics.[18] After pyrolysis, NMR studies showed that the aluminium was present as AlN_4, AlN_5 and AlN_6 units and the material was carbon free. The crystallisation of AlN from the amorphous matrix is an obvious concern since the Al^{3+} ions will be much more mobile than the Si^{4+} at 1000 °C, however there was no evidence of phase segregation from PXD or TEM data.

Kaskel has similarly developed a single source precursor to Si/Al/N compositions from the reactions of $Si(NHEt)_4$ with trimethyl- or triethyl-aluminium, Fig. 8.[19] However, reactions with ammonia at atmospheric pressure led to materials with highly depleted Si content and $Si(NHEt)_4$ was detected in the gaseous by-products. The higher reactivity of the Al centre was believed to have caused sequential reactions, with Al reacting first then Si. Ammonolysis in supercritical NH_3 was needed to achieve materials with close to a 1 : 1 Al : Si ratio and these were homogeneous on the lengthscale of an EDX experiment. No attempt to control gelation was made and this material was obtained as flakes. However, these had a surface area of 760 m^2g^{-1} and proved effective at catalysing the Michael addition of malonitrile to acrylonitrile (96% conversion in 5 h).

Two groups have also incorporated transition metals into silicon nitride using a sol–gel approach. Jansen[20] investigated the reactivity of a series of amides with ammonia by NMR to find combination which had similar reaction rates. If rates of ammonolysis and condensation are similar, the probability of forming M–NH–Si linkages is similar to that of forming

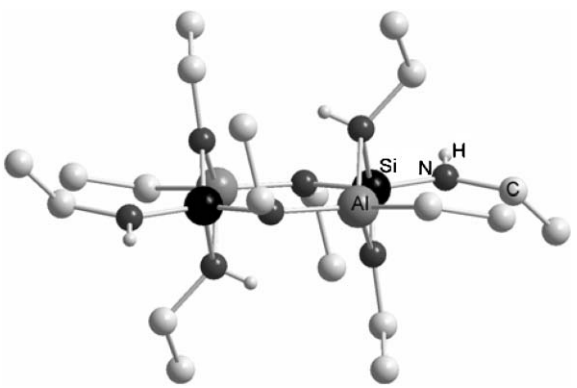

Fig. 8 Crystal structure of $[EtAl(\mu\text{-}NHEt)(\mu\text{-}NEt)_2Si(NHEt)]_2$.[19] Ethyl group hydrogen atoms omitted for clarity.

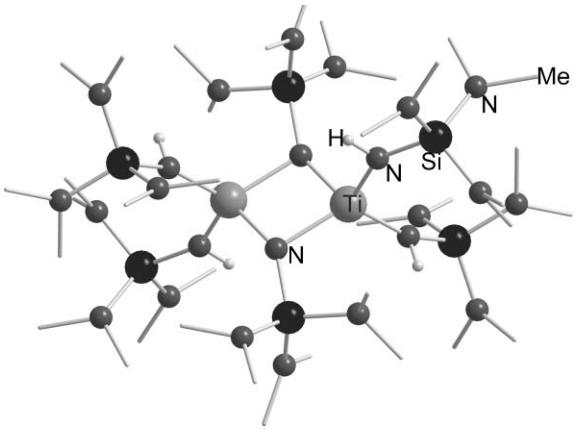

Fig. 9 Crystal structure of $[Ti(\mu\text{-}NSi(NMe_2)_3)(NHSi(NMe_2)_3)_2]_2$.[21] Methyl group atoms have been omitted for clarity.

Si–NH–Si or M–NH–M and the gels produced should contain a homogeneous distribution of M and Si. The purpose was to improve fracture strength and resistance to oxidation or thermal shock.

$Ti(NMe_2)_4$, $Zr(NMe_2)_4$ and $Ta(NMe_2)_5$ were found to have similar ammonolysis rates to $Si(NHMe)_4$.[20] Mixed solutions of metal and silicon amide were exposed to ammonia in solution and the resulting gels pumped to dryness. These were heated to 1000 or 1500 °C under NH_3. At 1000 °C the Ti/Si and Zr/Si materials were amorphous, whereas TaN had begun to crystallise at this temperature in the Si/Ta material. At 1500 °C all three were composites of MN nanocrystals and an amorphous M/Si/N matrix. The crystallisation of the metal nitride reflects the higher mobility of the metal ions in a nitride lattice compared with the small, covalently bound silicon atom. Such composites are of interest as hard materials since the movement and growth of dislocations in the hard, nanocrystalline phase are inhibited by the amorphous phase.

An alternative approach[21] has been to react the compound shown in Fig. 9 with NH_3 in an autoclave, yielding a silicon titanium imide powder. Pyrolysis under ammonia at 1000 °C yielded a mesoporous material which X-ray diffraction showed to contain TiN nanocrystals, similarly to the material produced by Jansen.

$[Ti(\mu\text{-}NSi(NMe_2)_3)(NHSi(NMe_2)_3)_2]_2$ was reacted with ammonia in an autoclave because it was found to be insoluble. However, it was produced by the decomposition over several days of $Ti(NHSi(NMe_2)_3)_4$,[21] which was soluble in organic solvents. Hence there is also the potential to carry out sol–gel processing with this compound.

Mesoporous Pd/Si_3N_4 nanocomposites have been produced by reaction of a pre-formed silicon diimide gel (from $Si(NH_2)$-$(SiNMe_2)_3$ as described in section 3) with $PdCl_2$, followed by ammonia pyrolysis.[22] These were shown to be active for hydrogenation and hydrogen transfer reactions with alkenes.

5. Nitrides of elements other than silicon

5.1 Boron and gallium nitrides

Hexagonal boron nitride (h-BN), which has a graphite-like structure, is a very lightweight ceramic that is useful as an

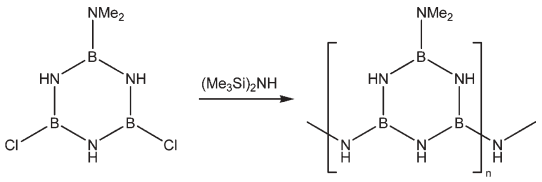

Fig. 10 Borazine crosslinking by hexamethyldisilazane.[23]

electrical insulator but can also be machined to yield shaped pieces. The cubic (diamond-structured) modification is extremely hard. The nitrides of the heavier group 13 elements aluminium, gallium and indium are important semiconductor materials, especially for light emission.

Paine used sol–gel methods to produce h-BN as films and aerogels as discussed in a previous review.[23] Cyclic chloroborazines were found to be readily cross linked by $(Me_3Si)_2NH$ with evolution of Me_3SiCl and the reaction in Fig. 10, carried out in chlorobenzene or without solvent, yielded gels that were transformed to glassy solids on solvent removal. Pyrolysis of these in NH_3 led to h-BN. However, these materials lacked processibility.

Crosslinking of the $[(BCl)(NH)]_3$ cyclic borazine with $(Me_3Si)_2NH$ resulted in gels in a variety of solvents.[23] Coatings could be deposited prior to gelation and pyrolysis under N_2 or NH_3 led to h-BN films. Pyrolysis under N_2 led to small quantities of Si contamination, but this was avoided with NH_3. Critical point drying of the gels in CO_2, followed by pyrolysis at 1200 °C led to aerogel monoliths with surface areas of 200–400 m^2g^{-1} (this material is of very low density). These could also be densified with shape retention at higher temperatures.

Dissolution of the $[(BCl)(NH)]_3/(Me_3Si)_2NH$-derived xerogels in liquid ammonia also resulted in solutions from which fibres could be drawn. The liquid ammonia removes some crosslinks rendering the material soluble. Drying these solutions then redissolving in an organic solvent yielded solutions from which BN fibres and coatings could readily be produced.

Kroke[24] has employed the same $[(BCl)(NH)]_3$ precursor with the $(Me_3Si)_2NCN$ reagent used for crosslinking of silicon carbodiimide gels as described in Scheme 2. Xerogels were formed by warming these in THF or toluene. Pyrolysis under dry Ar at 1200 °C resulted in an amorphous ceramic of approximate composition B_4CN_4. Structurally this was considered to be a turbostratic BN phase, largely a graphite-type structure but with disordered layers. Between 1800 and 2000 °C this phase loses N_2 yielding B_4C, an important hard material for applications such as armour plating and blasting nozzles.

Reactions of $Ga_2(NMe_2)_6$ with ammonia[25] are a direct analogue of sol–gel type processes, Scheme 3. These reactions were used to produce powdered materials, however these were porous with high surface areas. It was found to be possible to produce microporous materials by including long chain amines

$$Ga_2(NMe_2)_6 \xrightarrow{NH_3} Ga(NH)_x(NH_2)_y(NMe_2)_z \xrightarrow{heat} GaN$$

Scheme 3 A sol–gel process for gallium nitride.[25]

in the mixtures as discussed in section 3.2 for $Si(NMe_2)_3(NH_2)$-derived gels. The mobility of Ga^{3+} is higher than that of Si^{4+} and crystallisation to cubic or hexagonal GaN is observed above 400 °C. However differences in the products with or without an amine template were observed even after heating to 800 °C. The non-templated structures formed micron-sized crystallites, whereas nonylamine-templated GaN was found to be nanocrystalline with an average crystallite size of 9 nm. The mesopores in this material were found to increase in size with pyrolysis temperature and the small size of the eventual crystallites was attributed to the thin walls that provide the feedstock for crystallisation, or to surface impurities associated with the template molecules (though the bulk composition was very similar to the non-templated materials).

5.2 Sol–gel routes to nitrides of d-block metals

Transition metal nitrides are of interest for a broad spectrum of applications including their well established uses as barrier layers for electronics and hard, low friction materials but also as catalysts, photocatalysts, magnetic materials, biocompatible coatings and electrical contacts.

Reactions of metal dialkylamides and bis(trimethylsilyl)-amides with ammonia were examined in detail by Chisholm,[26] following earlier work by Brown and Maya.[27] These reactions led to powdered products and no attempt was made at applying sol–gel processing techniques.

However, these studies demonstrated the general applicability of this chemistry to produce metal nitrides with a wide range of metals, Table 2. Note that at the high temperatures used the thermodynamically stable phases were obtained. TGA data showed that these materials formed in two steps. At low temperature, dimethylamine and ammonia were lost, corresponding to the decomposition of NH_2 and NMe_2 groups. Sometimes N_2 was also lost at this stage. In cases where a reduction in the metal oxidation state is seen, a further high temperature N_2 loss was observed. Often there was a plateau in the mass traces at around 400–500 °C and these may have corresponded to higher nitride compositions, though no carbon analysis was carried out on the pyrolysed materials.

We recently re-examined[28] the ammonolysis of $Ti(NMe_2)_4$ and obtained carbonitrides by heating to the plateau in the weight loss trace, these lost N_2 with further heating to yield Ti(C,N) materials. Nonetheless, these were shown to be interesting as potential routes to ultrahard materials, since they tend to form nanocrystal/amophous composites.

Transition metals are larger and more electropositive than the p-block elements described in previous sections. Control of

Table 2 Metal nitrides produced by ammonolysis of amides followed by pyrolysis at 1000 °C in He[26]

Metal amide	Product by PXD
$M(NMe_2)_4$ (M = Ti, Zr, Hf, V) or $Nb(NEt_2)_4$	MN
$M(NMe_2)_5$ (M = Nb, Ta)	MN
$M(N(SiMe_3)_2)_3$ (M = Y, La, Ti, V)	MN
$Cr(N^iPr_2)_3$, $Cr_2(NEt_2)_4$, $Cr(NEt_2)_4$, $Cr(N(SiMe_3)_2)_3$	Cr_2N
$M_2(NMe_2)_6$ (M = Mo, W) or $W(NMe_2)_6$	M_2N
$Fe(N(SiMe_3)_2)_3$	Fe
$M(N(SiMe_3)_2)_2$ (M = Mn, Co)	M
$Cu(N(SiMe_3)_2)_2$	Cu_3N

$$Ti(NMe_2)_4 \xrightarrow{H_2N^n Pr} Ti(N^n Pr)_x(NH_n Pr)_y(NMe_2)_z \xrightarrow{heat} Ti(C,N)$$

Scheme 4 Primary amine based sol–gel route for titanium nitride.[30]

the condensation process is therefore significantly more difficult. In the $Ti(NMe_2)_4/NH_3$ system, we found that a combination of a bipyridyl reaction moderator, limited amounts of ammonia (2 molar equivalents) and low temperature did allow the formation of stable, brick red sols in THF.[29] These were opaque but could be filtered through a fine sinter and could be used to produce TiN coatings by dip coating. However, the coating quality was poor in terms of cracking and adhesion. Good coatings require condensation to occur as the solvent evaporates during the coating process, such that chemical bonds link particles within the film. It is likely these sols were stable simply because of small particle size and that all $Ti–NH_2$ groups underwent condensation during sol formation.

An alternative approach is to use a crosslinking agent that undergoes condensation less readily. We tried reactions of $Ti(NMe_2)_4$ with primary amines, Scheme 4, and found that, whilst excess amine led to precipitation, with smaller quantities this could be avoided. Two molar equivalents are needed to reach the theoretical endpoint of this process, $Ti(NR)_2$, but it was found that even with 3½ equivalents no precipitation occurs. Consumption of the amide and production of dimethylamine by-product were shown to occur quantitatively by NMR, so it is the condensation process that does not go to completion.

It was found to be possible to produce good quality films of nanocrystalline TiN or Ti(C,N) from this system by dip coating and pyrolysis in NH_3 or N_2 respectively. The use of $^nOctNH_2$ produced slightly smoother films, Fig. 11, though unsurprisingly with higher carbon content when pyrolysed in N_2. It may be that the longer chain amine resulted in larger pores and thus solvent could escape the coatings more readily. The films were highly conductive. With a sterically hindered amine such as $^tBuNH_2$ the amination process was found to be inhibited and this system did not yield films.

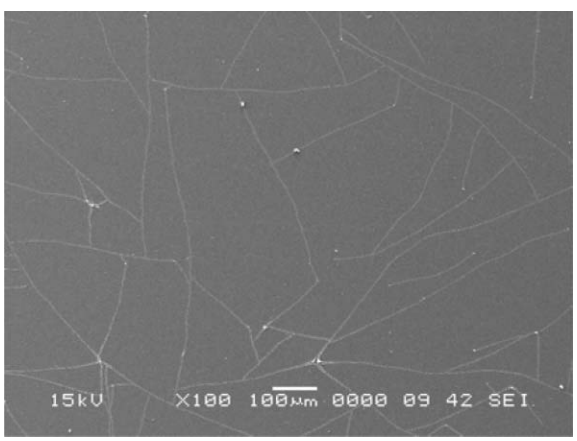

Fig. 11 SEM image of a Ti(N,C) film produced by dip-coating a $Ti(NMe_2)_4/^nOctNH_2$ sol then heating in N_2. Reprinted from ref. 30.

6. Sol–gel chemistry based on processing of sulfide and selenide nanoparticles

An alternative approach to the sol–gel processing of non-oxide materials has been developed by Boilot and Gacoin.[31] CdS nanoparticles were prepared with a capping agent that could be controllably removed. The –SPhF cap could be controllably oxidised by the addition of H_2O_2 yielding a soluble dithiol.

This partial removal of the capping agent leads to aggregation of the nanoparticles and, with appropriate quantities of oxidant, stable translucent gels can be obtained from acetone solutions of the nanoparticles. An excess of oxidant leads to precipitation whereas too little leads to stable sols. This is analogous to controlling gelation of alkoxide-derived sols through the amount of water added. Extended exposure of solutions of these nanoparticles to air could also eventually lead to sufficient oxidation to cause gelation.

Gels were produced from CdS nanoparticle solutions with concentrations ranging from 1 to 5 mol dm^{-3}.[31] After gelation, syneresis was observed with a 10-fold contraction in the size of monolithic gels produced from the least concentrated nanoparticle solutions.

It was also found to be possible to produce CdS films of controllable thickness (100–600 nm reported) by partially oxidising sols. The viscosity of the sols could be controlled by the degree of oxidation (*i.e.* the amount of H_2O_2 added) and these were spin-coated to yield transparent, crystalline films.

Brock has used supercritical drying to produce CdS aerogels from capped CdS nanoparticles according to the method described above.[32,33] Oxide aerogels, especially those of silica, have a wide variety of actual and potential applications as catalysts, sensors, thermal insulators, cosmic dust collectors and electrochemical device components. They are very low density materials formed by removing the solvent whilst leaving the pore network intact. Fig. 12 shows gels produced from 1 mol dm^{-3} solutions of CdS nanoparticles, note the difference in volume change between the two drying methods.

The range of materials which could be processed using these methods was also expanded by producing aerogels and xerogels of CdS, CdSe, ZnS and PbS.[32] The chemistry was changed slightly with CdSe. Here, nanoparticles were produced in trioctylphosphine oxide and capped with mercaptoundecanoic acid. Treatment with tetranitromethane led to opaque orange gels.

The gels consist of an assembly of linked particles, Fig. 13, which retain the pores that originally held the liquid. They have high surface areas and large pores, Table 3.

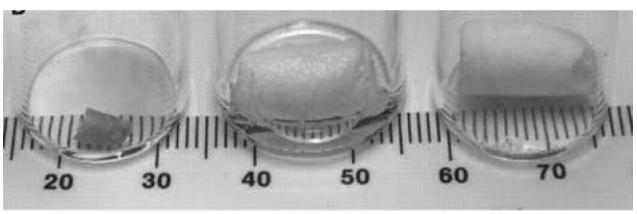

Fig. 12 Photographs showing a wet CdS gel (centre), a xerogel produced by air drying (left) and an aerogel dried in supercritical CO_2 (right). Reprinted with permission from ref. 31. Copyright (2001) AAAS.

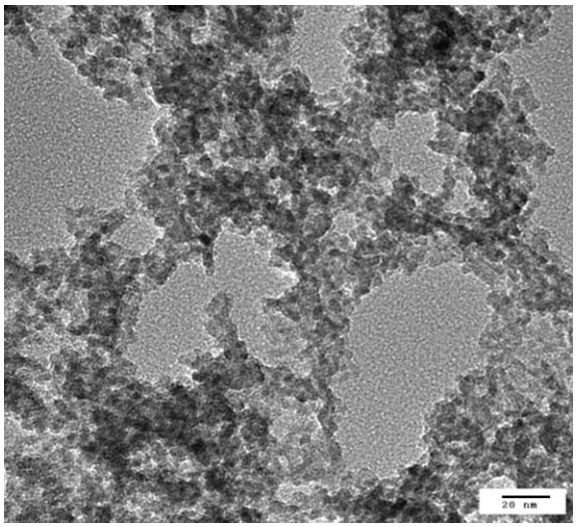

Fig. 13 Transmission electron micrograph of a CdSe aerogel showing linked nanoparticles and large pores. Reprinted with permission from ref. 33. Copyright (2006) American Chemical Society.

Table 3 Properties of semiconductor aerogels[32]

Aerogel	E_g (eV)[a]	Bulk E_g (eV)[a]	BET surface area (m^2g^{-1})	Average pore diameter (nm)
PbS	0.80	0.37	130	21–45
CdSe	2.19	1.74	143	16–29
CdS	2.71	2.42	245	29–30
ZnS	3.80	3.54	192	15–30

[a] Estimated from the low energy onset in absorbance curves based on diffuse reflectance spectra.

Despite their 3-dimensional connectivity, these aerogels retain some of the optical properties of the nanoparticles from which they are formed. Sharp absorption onsets are observed at significantly higher energy than the bandgaps of bulk crystalline samples of the semiconductors, Table 3. This is consistent with the retention of quantum confinement effects.

Unheated CdS aerogels did not exhibit band-edge emission, which was observed from the free nanoparticles.[32] Heating to 100 °C gave materials that did exhibit some band-edge emission, though some increase in the crystallite size was also observed. With CdSe, preparation of the nanoparticles at higher temperature did result in aerogels which exhibited band-edge emission.

7. Outlook and concluding remarks

It is clear that nitrides and chalcogenides derived using sol–gel chemistry have great potential and a great deal of further work is needed to exploit these materials.

A number of sol–gel derived nitride materials have been shown to be active catalysts (sections 3.2 and 4.2). However, most of the materials produced have not been investigated and the subtleties of selectivity that can be achieved by small variations in the pore size remain to be explored. Mixed element nitride systems have begun to be investigated and there is the possibility of combining catalytic activity of metal nitrides (*e.g.* Mo_2N) with the basic properties of the silicon nitride systems to yield new catalytic functionalities.

$$Ti(SR)_4 \xrightarrow{H_2S} Ti(S)_x(SH)_y(SR)_z \xrightarrow{heat} TiS_2$$

$$GaCl_3 \xrightarrow{(Me_3Si)_3P} Ga(P)_x(P(SiMe_3)_{1or2})_y(Cl)_z \xrightarrow{heat} GaP$$

Scheme 5 Possible reactions for sol–gel processing of useful materials.

Porous materials are one of the strengths of sol–gel methods generally and as well as membranes (section 3.1) it is likely that silicon and boron nitrides could find applications as insulators for extreme conditions.

Some groups have also begun to investigate the formation of materials with ordered pores. These could vary the catalytic properties of nitride materials or provide oxide free analogues of ordered meso- and macro-porous materials that are of intense interest for optical and electronic applications.

Jansen[34] has formed liquid crystal phases of cetyl- and dodecyl-trimethylammonium bromide in liquid ammonia with the expressed aim of templating mesoporous nitride based solids. Cheng *et al.*[35] produced porous silicon oxynitride glasses from the reaction of $Si(NMe_2)_3(NH_2)$ with formamide followed by pyrolysis. This complex reaction leads to gels containing Si–OC(H)N–Si, Si–N(CHO)–Si and Si–NH–Si linkages. The authors noted that since this chemistry could be carried out in a dimethylformamide solvent, templating structures around cationic surfactants such as cetyltrimethylammonium bromide was a possibility.

The properties of aerogels based on semiconductor nanoparticles (section 6) have only just begun to be investigated, but it is clear that these combine the properties of nanoparticles (emission, quantum confinement) with the physical state of bulk materials (monoliths, films). These may provide good heterogeneous photocatalytic systems. It should also be possible to produce composite materials based on these aerogels, *e.g.* by polymer infiltration, to combine their optical properties with greater mechanical stability.

Nanoparticles have been grown in many systems as well as group 12 and 14 chalcogenides. The gelation of nanoparticles by controlled agglomeration through the destabilisation of surface capping groups has the potential to provide the means to carry out sol–gel processing in a very large number of systems. This includes metals, elemental semiconductors, compound semiconductors and insulators. Hence this has the potential to develop into a strong and exciting area of materials chemistry.

Chemistries that could be used for controlled condensation reactions also exist for other anion species and could be developed to sol–gel processing methods, Scheme 5. Reactions of a series of titanium(IV) thiolates and of $Nb(SC_6H_3Me_2\text{-}2,6)_5$ with H_2S have been investigated[36] and lead to high quality MS_2 powders. The control of ligand substitution and condensation reactions are not easy. However, if these can be achieved the sol–gel process is adaptable to a wide range of nonoxide materials in new forms.

Acknowledgements

ALH is supported by a Royal Society University Research Fellowship. Thanks to Dr Fei Cheng and Dr Baishakhi Mazumder for helpful comments on the manuscript.

References

1 For a general description see *e.g.* U. Schubert, and N. Hüsing, Synthesis of Inorganic Materials, 2nd edition, pp. 192–221 and references on pp. 233–234, Wiley-VCH, Weinheim, 2005.
2 H. Yamamura, M. Yamamoto and K. Kakinuma, *J. Ceram. Soc. Jpn.*, 2005, **113**, 458.
3 K. Nakane, N. Ogata and Y. Kurokawa, *J. Appl. Polym. Sci.*, 2006, **100**, 4320.
4 I.-S. Kim and P. N. Kumta, *J. Mater. Chem.*, 2003, **13**, 2028 and references therein.
5 S. J. Henderson and A. L. Hector, *J. Solid State Chem.*, 2006, **179**, 3518.
6 J. Löffelholz, J. Engering and M. Jansen, *Z. Anorg. Allg. Chem.*, 2000, **626**, 963.
7 R. Rovai, C. W. Lehmann and J. S. Bradley, *Angew. Chem., Int. Ed.*, 1999, **38**, 2036.
8 F. Cheng, S. J. Archibald, S. Clark, B. Toury, S.M. Kelly and J. S. Bradley, *Chem. Mater.*, 2003, **15**, 4651 and ref. 13 therein.
9 C. Balan, K. W. Völger, E. Kroke and R. Riedel, *Macromolecules*, 2000, **33**, 3304 and references therein.
10 F. Cheng, S. M. Kelly, S. Clark, J. S. Bradley, M. Baumbach and A. Schütze, *J. Membr. Sci.*, 2006, **280**, 530.
11 K. W. Völger, R. Hauser, E. Kroke, R. Riedel, Y. H. Ikuhara and Y. Iwamoto, *J. Ceram. Soc. Jpn.*, 2006, **114**, 567.
12 S. Kaskel, K. Schlichte and B. Zibrowius, *Phys. Chem. Chem. Phys.*, 2002, **4**, 1675 and references therein.
13 D. Farruseng, K. Schlichte, B. Spliethoff, A. Wingen, S. Kaskel, J. S. Bradley and F. Schüth, *Angew. Chem., Int. Ed.*, 2001, **40**, 4204.
14 Q. Dat Nghiem, J.-K. Jeon, L.-Y. Hong and D.-P. Kim, *J. Organomet. Chem.*, 2003, **688**, 27 and references therein.
15 R. Riedel, G. Mera, R. Hauser and A. Klonczynski, *J. Ceram. Soc. Jpn.*, 2006, **114**, 425 and references therein.
16 A. Hannemann, J. C. Schön and M. Jansen, *J. Mater. Chem.*, 2005, **15**, 1167 and refs 26–27 therein.
17 M. Weinmann, R. Haug, J. Bill, M. de Guire and F. Aldinger, *Appl. Organomet. Chem.*, 1998, **12**, 725.
18 F. Cheng, S. M. Kelly, F. Lefebvre, S. Clark, R. Supplit and J. S. Bradley, *J. Mater. Chem.*, 2005, **15**, 772.
19 S. Kaskel, G. Chaplais and K. Schlichte, *Chem. Mater.*, 2005, **17**, 181.
20 J. Engering and M. Jansen, *Z. Anorg. Allg. Chem.*, 2003, **629**, 913 and ref. 9 therein.
21 F. Cheng, S. M. Kelly, S. Clark, N. A. Young, S. J. Archibald and J. S. Bradley, *Chem. Mater.*, 2005, **17**, 5594.
22 F. Cheng, S. M. Kelly, N. A. Young, C. N. Hope, K. Beverly, M. G. Francesconi, S. Clark, J. S. Bradley and F. Lefebvre, *Chem. Mater.*, 2006, **18**, 5996.
23 R. T. Paine and C. K. Narula, *Chem. Rev.*, 1990, **90**, 73 and references therein.
24 K. W. Völger, E. Kroke, C. Gervais, T. Saito, F. Babonneau, R. Riedel, Y. Iwamoto and T. Hirayama, *Chem. Mater.*, 2003, **15**, 755.
25 G. Chaplais and S. Kaskel, *J. Mater. Chem.*, 2004, **14**, 1017.
26 D. V. Baxter, M. H. Chisholm, G. J. Gama, V. F. DiStasi, A. L. Hector and I. P. Parkin, *Chem. Mater.*, 1996, **8**, 1222.
27 G. M. Brown and L. Maya, *J. Am. Ceram. Soc.*, 1988, **71**, 78.
28 A. W. Jackson, O. Shebanova, A. L. Hector and P. F. McMillan, *J. Solid State Chem.*, 2006, **179**, 1383.
29 A. L. Hector and A. W. Jackson, *Proc. Mater. Res. Soc.*, 2005, **848**, FF2.2.1.
30 A. W. Jackson and A. L. Hector, *J. Mater. Chem.*, 2007, **17**, 1016.
31 T. Gacoin, K. Lahill, P. Larregaray and J.-P. Boilot, *J. Phys. Chem. B*, 2001, **105**, 10228 and references therein.
32 J. L. Mohanan, I. U. Arachige and S. L. Brock, *Science*, 2005, **307**, 397.
33 I. U. Arachchige and S. L. Brock, *J. Am. Chem. Soc.*, 2006, **128**, 7964 and references therein.
34 S. Bzik and M. Jansen, *Chem.–Eur. J.*, 2003, **9**, 614.
35 F. Cheng, S. M. Kelly, F. Lefebvre, A. F. Lee, K. Wilson, S. Clark and J. S. Bradley, *J. Mater. Chem.*, 2005, **15**, 3039.
36 C. J. Carmalt, C. W. Dinnage, I. P. Parkin, A. J. P. White and D. J. Williams, *Inorg. Chem.*, 2002, **41**, 3668.